OPTICAL REVIEW Vol. 17, No. 3 (2010) 341–345

Visible Nonlinear Band-Edge Luminescence in ZnSe and CdS Excited by a Mid-Infrared Free-Electron Laser

Eiji TOKUNAGA[1,2,3*], Naoto SATO[1], Jiro KORENAGA[1], Takayuki IMAI[3], Shin SATO[4], and Hiro-o HAMAGUCHI[4]

[1]*Department of Physics, Faculty of Science, Tokyo University of Science, 1-3 Kagurazaka, Shinjuku, Tokyo 162-8601, Japan*
[2]*Research Center for Green Photo-Science and Technology, Tokyo University of Science, 1-3 Kagurazaka, Shinjuku, Tokyo 162-8601, Japan*
[3]*Infrared Free Electron Laser Research Center, Research Institute for Science and Technology, Tokyo University of Science, 2641 Yamazaki, Noda, Chiba 278-8510, Japan*
[4]*Department of Chemistry, School of Science, University of Tokyo, 7-3-1 Hongo, Bunkyo, Tokyo 113-0033, Japan*

(Received September 19, 2009; Accepted December 15, 2009)

Visible nonlinear band-edge luminescence in ZnSe and CdS bulk crystals was observed upon excitation by a mid-infrared free-electron laser (mid-IR FEL) at approximately 9 μm. The emission intensity is proportional to the 74th and 45th powers of the excitation intensity for ZnSe and CdS, respectively. For ZnSe, the temporal profile of the emission intensity does not follow the profile of the excitation macropulse of the FEL, but sharply rises and decays only at the maximum of the macropulse profile. These features are in marked contrast to those of a previous report, where the emission profile follows that of the macropulse, and the emission intensity scales with the 4th power of the excitation intensity. The experimental observations were reproduced by a numerical simulation based on impact ionization and avalanche ionization by electrons accelerated by the optical electric field of the FEL. The large nonlinearity in the band-edge emission comes from the macropulse temporal structure, which consists of micropulses densely spaced to allow excited carriers to survive when the next micropulse arrives. They work as seed carriers in the next carrier multiplication step.

Keywords: free electron laser, mid infrared, semiconductor, upconversion, optical nonlinearity, bandedge luminescence, impact ionization, ponderomotive potential, ZnSe, CdS

1. Introduction

Upconversion of photon energy is an interesting and useful phenomenon. In the solid state, harmonic generation with a nonlinear crystal and multistep excitation in a rare-earth-ion-doped solid are well known and widely used for near-IR to visible upconversion. However, there is no commercial solid material for mid- or far-IR to visible upconversion, except for materials with photo-stimulated luminescence or thermal luminescence, which is not an intrinsic upconversion process. In the gas phase, by contrast, radio frequency- or microwave- gas discharge plasma readily radiates visible plasma luminescence from ionized gases, which are excited by impact ionization of electrons accelerated by the electric field of the applied electromagnetic waves. If this is regarded as a photon upconversion process, the photon energy is multiplied by more than 10^5 times from microwave or radio-frequency photons to visible photons. This is a remarkable upconversion process.

In the solid phase, impact ionization due to electrons accelerated by an intense optical electric field usually leads to laser-induced breakdown.[1)] However, if stable, reproducible, and efficient luminescence can be observed by this process in a solid, it is usable for a new upconversion material. In fact, upon excitation by a mid-IR free-electron laser (FEL), band-edge luminescence was previously observed in various semiconductors at low temperature,[2)] and in ZnSe at room temperature.[3)] Luminescence from laser ablation plasma in a solid[4)] at room temperature was also reported. The mechanism underlying such luminescence is understood as follows. Ionization of bound electrons in a solid, i.e., interband excitation of electrons from valence band to conduction band, occurs through impact ionization due to electrons accelerated by an optical electric field. This is similar to visible plasma emission from an ionized gas irradiated by a microwave. However, the microscopically detailed mechanisms are not fully understood because it is so complicated a process, and there still remain many unknown physical quantities such as photon conversion efficiency. As a consequence, the possibility for application is yet to be fully explored.

In this study, we observed band-edge luminescence in ZnSe and CdS under excitation by an intense mid-IR FEL at the Tokyo University of Science (FEL-TUS),[5)] but the excitation intensity dependence and temporal behavior of the luminescence were very different from those in previous reports.[2,3)] We analyzed the results on the basis of the FEL pulse characteristics different from those for the Osaka FEL[6)] used in refs. 2–4.

2. Experimental

The FEL can deliver widely tunable IR pulses with high peak power and relatively narrow bandwidth, so that it is an ideal optical source to study the effect of high-density resonant excitation of low-energy elementary particles such as optical phonons in condensed matter. The experiments were performed at the Infrared FEL Research Center at the TUS, Japan.[5,7,8)] The FEL-TUS delivers laser pulses with wavelengths between 5 and 14 μm and a temporal width of about 2 μs, and is operated at 5 Hz in the present experiment.

*E-mail address: eiji@rs.kagu.tus.ac.jp

Typically, the FEL pulse has a bandwidth of about $18\,cm^{-1}$ at full width at half maximum (FWHM). With regard to the pulse structure of the FEL-TUS, the macropulses consist of a train of micropulses. Micropulses are of 2 ps duration, 2856 MHz repetition, and 2–5 MW peak power. Macropulses are of 2 μs duration, 5 Hz repetition, and 150 mJ energy.

Before being irradiated onto a sample, part of the FEL pulses were split by a CaF_2 beamsplitter into an MCT detector (Boston Electronics PD-10.6-3, response time <1 ns) to monitor the temporal structure of macropulses. FEL pulses were focused onto the sample by an $f = 10$ mm ZnSe lens with a spot size of 0.35 mm. Emissions from the sample were delivered through a fiber bundle to a monochromator and the emission spectra were detected by a CCD with an image intensifier (ICCD; Oriel MS257). To increase the signal-to-noise (S/N) ratio, the ICCD was under gated operation triggered by delay-controlled pulses, which were synchronized with macropulses.

For time-resolved measurement, emission signals were detected by an Si-APD (Hamamatsu S5343) and temporally dispersed by a 500 MHz oscilloscope, together with FEL macropulse signals, which were detected by the MCT along the same time axis. The time resolution was estimated to be 10 ns at most.

Samples used were undoped ZnSe(110) and CdS(110) single crystals of $5 \times 5\,mm^2$ (Techno Chemics). The experiments were performed at room temperature.

3. Results and Discussion

3.1 Band-edge emission

Figure 1 shows emission spectra for ZnSe and CdS excited by 9 μm FEL pulses. For comparison, emission spectra due to interband excitation with a 441.6 nm HeCd laser (Kimmon) at room temperature are also shown. For both samples, the emission peaks are slightly below the band-gap (ZnSe: 2.7 eV, CdS: 2.4 eV). To observe visible band-edge emissions by FEL excitation, the excitation intensity must be carefully adjusted by moving the focus lens to defocus the laser beam slightly. If focused tightly, brighter white emissions were observed accompanied by laser ablation to leave a permanent destructive spot in the crystal.[4] Thus, this emission can be called destructive emission. In general, it was much easier to observe the destructive emission than the band-edge emission. The band-edge emission was only observed on the conditions that both the temporal profile and intensity of the FEL macropulse were good, an irradiated spot on the sample surface was carefully selected, and the beam was slightly defocused.

For both samples, the band-edge emissions were redshifted for FEL excitation with respect to those for HeCd excitation. This is considered to be caused by a redshift of the band-gap due to an increase in sample temperature caused by FEL irradiation. On the basis of ref. 9, the temperature dependence of band-gap energy from 50 to 200 K was linearly extrapolated above 300 K. Then, we obtained an estimated value for the temperature increase in ZnSe caused by FEL excitation of 150 °C.

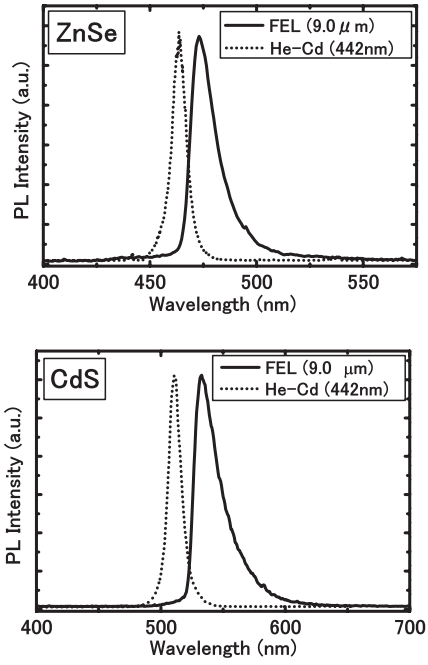

Fig. 1. Emission spectra for ZnSe and CdS excited by 9 μm FEL pulses (solid curves) and by a 441.6 nm HeCd laser (dotted curves) at room temperature.

3.2 Excitation-intensity dependence

Figures 2(a) and 2(b) show the excitation-intensity dependence of the emission intensity at 9 μm. For ZnSe and CdS, the emission intensity is proportional to the 74th and 45th powers of the excitation intensity, respectively. The 74th power dependence means that a 10% increase in the excitation intensity leads to a 1000 times increase in the emission intensity. If multiphoton excitation were a mechanism for the band-edge emission, 20 and 17 photons of 0.138 eV (9 μm) are sufficient to reach the band-gap energy for ZnSe (2.7 eV) and CdS (2.4 eV), respectively. Thus, the 20th and 17th power dependences for ZnSe and CdS, respectively, are expected. However, the experiments show much higher power dependences. This indicates that multiphoton excitation is not a mechanism of the band-edge luminescence. This is supported by absence of an intense absorption band between 0.138 eV and the band-gap energy for both samples, which makes multiphoton excitation unlikely to occur because of the absence of any resonant intermediate levels.

3.3 Excitation-wavelength dependence

Figure 3 shows the excitation-wavelength dependence of the emission intensity for ZnSe. The dependence shows complicated behavior due to the strong excitation-intensity dependence at the same wavelength. The graph shows that if the excitation intensity is the same between two wavelengths, the emission intensity is larger for the longer wavelength. In other words, the emission intensity increases with decreasing photon energy. At the same wavelength, a slight decrease in the excitation intensity leads to a substantial decrease in the emission intensity, consistent with the strong excitation-intensity dependence.

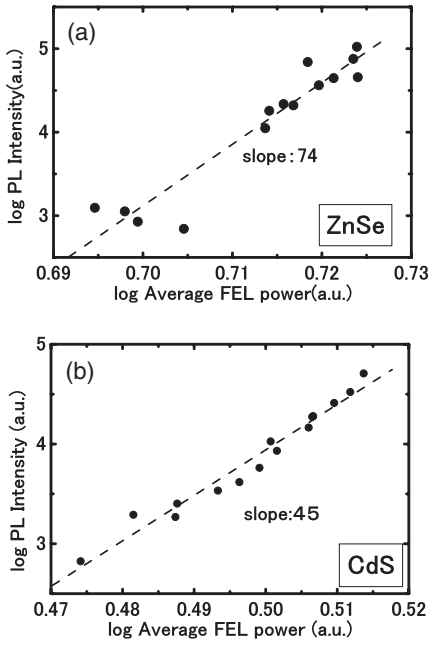

Fig. 2. Excitation-intensity dependence of the emission intensity excited at 9 μm for ZnSe (a) and CdS (b).

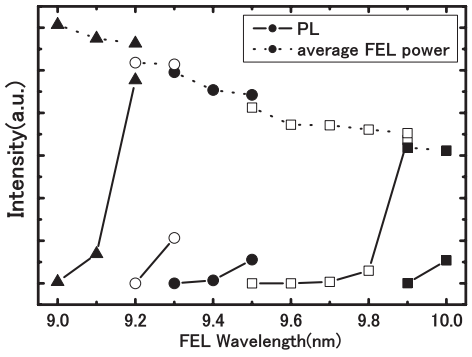

Fig. 3. Excitation-wavelength dependence of the emission intensity for ZnSe. The dependence shows complicated behavior due to the strong excitation-intensity dependence at the same wavelength. The graph shows that the emission intensity increases with decreasing photon energy.

This behavior contradicts multiphoton excitation. It is strongly suggested that the ponderomotive potential due to the field of FEL pulses plays an essential role in the band-edge emission through impact ionization.[10,11] When an electron of effective mass m and charge $-e$ is under an oscillating electric field of $E = E_0 \sin \omega t$, the cycle average of the kinetic energy of the electron is given by the ponderomotive potential[12]

$$U_p = \frac{e^2 E_0^2}{4m\omega^2}. \quad (1)$$

The accelerated electron collides with a constituent atom in the crystal and ionizes it to release a free electron, or, in other words, to excite a valence electron to the conduction band. This electron is accelerated in the same manner. This

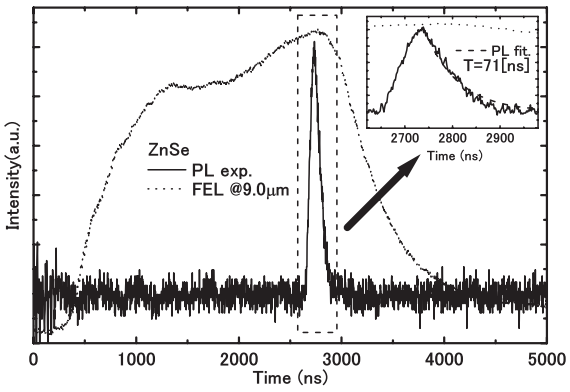

Fig. 4. Temporal profiles of the emission intensity and of the 9 μm macropulse that excites ZnSe. Inset: time evolution of the emission intensity on the expanded time scale around the later peak of the macropulse.

elementary process occurs repeatedly to result in avalanche ionization, i.e., the population of free electrons increases explosively to give visible emissions in the relaxation process, or excessive heating leading to destruction of the crystal structure. The wavelength dependence of the emission intensity reflects the ω dependence of U_p.

3.4 Temporal evolution of the bandedge emission

Figure 4 shows the temporal profiles of the emission intensity and of the 9 μm macropulse, which excites ZnSe. The emission intensity does not follow the macropulse profile temporally, but is concentrated only at the peak of the macropulse. The inset in Fig. 4 shows the time evolution on the expanded time scale around the peak of the macropulse. The apparent decay time of the emission was determined as 71 ns by fitting. It is known that the band-edge emission in ZnSe at room temperature is due to donor-to-free-hole transition.[13] The observed decay time is much longer than the reported decay times of 100 ps[14] and 3 ns[3] for this process. This is because the macropulse consisits of a train of micropulses separated by 350 ps periods. Carriers excited by impact ionization do not relax completely for one micropulse duration of 2 ps, but part of them survive when the next micropulse arrives, as expected from the 3 ns decay time. The residual carriers work as seeds for the avalanche ionization process for the next micropulse duration to result in the apparent extended decay time.

4. Model Calculation

To reproduce the temporal evolution of the emission intensity, we performed a simulation based on the scenario presented above. As a model for the visible band-edge emission, we adopted the electron–hole pair generation process due to interband excitation by impact ionization under the strong optical electric field.

Although undoped crystals were used, there exist impurity levels to allow for the presence of a significant amount of electrons thermally excited in the conduction band at room temperature. These electrons are accelerated by the ponder-

omotive potential due to the optical electric field of the FEL pulses. Then, the accelerated electrons collide with atoms and excite electrons in the valence band to the conduction band (impact ionization). The excited electrons are accelerated and collide with other electrons. This process is repeated, leading to avalanche ionization.[10,15] A large number of electron–hole pairs are generated and the band-edge emissions are observed as they are relaxed.

4.1 Recurrence relation of carrier population

The simulation was performed as follows. Considering that the micropulse duration is 2 ps, its repetition period is 350 ps, and the relaxation time is 3 ns,[3] it is reasonable to assume that the carrier acceleration and excitation processes occur instantaneously at the arrival of the delta-function pulse; then, the interband relaxation process occurs until the next pulse arrives. Here, intraband relaxation is assumed to be terminated within the pulse duration. The arrival times of a train of micropulses are numbered from the first as $t = 0, t_1, t_2, \ldots$. Similarly, the density of carriers $N(t_n)$ in the conduction band immediately before the arrival of the $n+1$-th micropulse at t_{n+1} can be treated as a sequence of numbers defined by the following recurrence relation.

$$N(t_{n+1}) = [N(t_n) + QN(t_n) - N(0)](1 - P) + N(0) \quad (2)$$

Here, $N(0)$ is the density of thermally excited initial carriers, $QN(t_n)$ is newly excited carriers by interband excitation due to Coulomb collision with the accelerated carriers $N(t_n)$ with $0 < Q < 1$, and P is the relaxation probability of each carrier before the next pulse arrives. Only a small part of the accelerated carriers can ionize the valence electrons. Note that the number of thermally excited initial carriers $N(0)$ does not contribute to the emission because they are originated from donor levels. At least this number of carriers is preserved in the conduction band throughout the process.

The n-th emission intensity at t_n is given by

$$I_{\mathrm{PL}}(t_n) = P[N(t_n)(1 + Q) - N(0)]. \quad (3)$$

This equation means a 100% emission quantum yield, but even if a realistic value for the yield is assumed such that P is replaced by yP with $0 < y < 1$, it does not change the emission intensity profile.

P can be expressed by a decay rate constant γ as follows. The relaxation process without the excitation process follows the differential equation

$$\frac{dN(t)}{dt} = -\gamma N(t) \quad (4)$$

to give the solution

$$N(t) = N_0 e^{-\gamma t}. \quad (5)$$

The relation between P and $N(t)$ is

$$N(t + \Delta t) = (1 - P)N(t), \quad (6)$$

where $\Delta t = 0.35$ ns (repetition period of micropulses). From eqs. (5) and (6), we obtain

$$P = 1 - e^{-\gamma \Delta t} = 1 - e^{-\Delta t/\tau}. \quad (7)$$

QN is the number of electrons in the conduction band excited by impact ionization with N electrons accelerated by the electric field as seeds. Thus $1 + Q$ is the magnification factor of the electron density at each step in the conduction band. We assumed simply that

$$Q(t) = CI_{\mathrm{FEL}}(t), \quad (8)$$

where I is the FEL intensity and C is an adjustable parameter. $I(t_n)$ was taken as a value for the temporal profile of the macropulse intensity at $t = t_n$ observed in Fig. 4.

Equation (2) represents the process for $I > I_{\mathrm{th}}$ (threshold intensity defined in the next subsection), while for $I < I_{\mathrm{th}}$ the recurrence relation is reduced as follows with $Q = 0$ in eq. (2).

$$N(t_n) = [N(t_{n-1}) - N(0)](1 - P) + N(0). \quad (9)$$

The emission intensity is expressed in the same manner as in eq. (3) with $Q = 0$. If eq. (9) is rewritten as $N(t_n) - N(0) = [N(t_{n-1}) - N(0)](1 - P)$, we obtain the solution for $N(t) - N(0)$, which decays exponentially as expected.

4.2 Ponderomotive potential

The maximum optical electric field of the FEL micropulse in the crystal is estimated to be 2×10^6 V/cm for the maximum excitation intensity of 2 GW/cm^2. The estimated value for the resulting ponderomotive potential in the experiment is 0.3 eV at largest. This is much lower than the band-gap energy of 2.7 eV for ZnSe, thus it appears that acceleration of electrons above the band-gap energy is unlikely to occur. As discussed in ref. 16, however, there exists a mechanism to accelerate electrons above U_{p} efficiently in a semiconductor as follows. Since the optical electric field changes its sign at the optical frequency, electrons cannot be continuously accelerated in the same direction but only reach the PM potential energy. In a semiconductor, however, the accelerated electron is subject to phonon scattering and the direction of its velocity is changed. If this occurs at a reasonable rate relative to the optical frequency, the velocity of an electron in the direction of the optical electric field is frequently reset to about zero for an electron to receive positive work continuously. As a result, the average kinetic energy of electrons in the condcution band can be much larger than the PM potential. In fact, we performed a Monte Carlo simulation for this process to confirm that electrons can obtain more than 3 eV kinetic energy within 2 ps (micropulse duration). Here, the scattering period was assumed to be 10 fs, i.e., scattering occurs about three times within a single period (30 fs) of the FEL optical field at 9 μm.

For impact ionization to take place, there should exist a certain threshold value in the intensity of the FEL macropulse. This is because if the macropulse intensity $I(t)$ is low, electrons cannot be accelerated above the band-gap energy even with the above mechanism. Therefore, we set a certain threshold value I_{th} for the intensity I such that $Q > 0$ only when $I > I_{\mathrm{th}}$.

4.3 Calculated results

Figure 5(a) shows the calculated result with appropriate

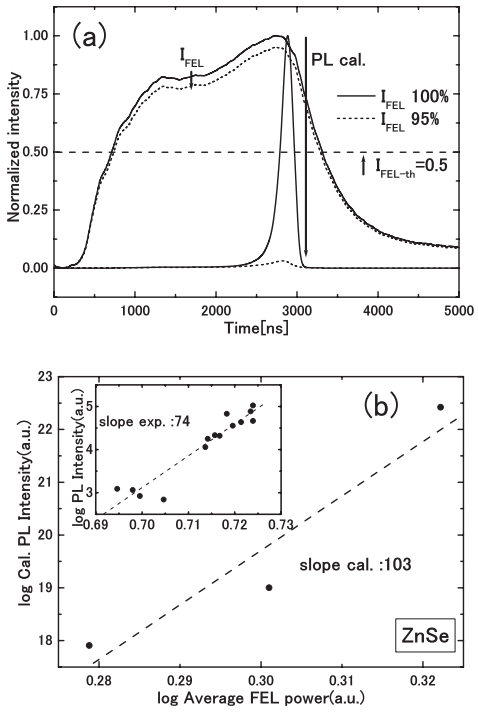

Fig. 5. (a) Solid curves: temporal profile of the emission intensity calculated for the macropulse of the structure shown in Fig. 4, with three adjustable parameters of C, I_{th}, and $N(0)$. The FEL macropulse intensity was normalized to the maximum intensity. Dashed curves: temporal profiles of the FEL macropulse whose intensity is reduced to 95% and of the emission intensity calculated from the reduced excitation intensity. (b) Excitation intensity dependence of the emission intensity calculated with the same parameters to give the result in (a).

parameters. There are three adjustable parameters of C, I_{th}, and $N(0)$. The calculation was made with $C = 0.128$, $I_{th} = 0.5$, and $N(0) = 10^{14}$. τ was taken to be 3 ns from the experiment in ref. 3 and the FEL macropulse intensity was normalized to the peak intensity. Agreement between the experimental and calculated results is fairly good. Among the four parameters (C, I_{th}, $N(0)$, and τ), only C and τ are sensitive to the relative shape of the emission temporal profile. Since τ is fixed by the experiment, this is practically fitting with one adjustable parameter, as long as the absolute value for the carrier density is not known experimentally. The calculated decay time (T_{cal}) is 66 ns, in agreement with the observed decay time of $T_{exp} = 71$ ns. T_{cal} is much longer than the intrinsic decay time of 3 ns that is used for calculation. This verifies the mechanism to give the longer decay time: Excited carriers do not completely relax but a part of them suvive when the next micropulse arrives to affect the apparent decay time.

As shown by the dashed curves in Fig. 5(a), if the FEL intensity is reduced to 95%, the emission intensity is reduced by two orders of magnitude compared with the case for 100% intensity. Figure 5(b) shows the excitation intensity dependence of the emission intensity calculated with the same parameters to give the result in Fig. 5(a). In this calculation, the relative emission intensity spans from 10^{-2} to 10^{+2} as the excitation intensity is varied from $100 - 5\%$ to $100 + 5\%$. The former is proportional to the 103rd power of the latter, in close agreement with that in Fig. 2(a).

5. Conclusions

We observed the highly nonlinear band-edge emission in ZnSe and CdS upon excitation of mid-IR FEL pulses. It was confirmed that impact ionization due to electrons accelerated by the optical electric field of the FEL is the mechanism for the emission. High orders of nonlinearity seen in the excitation intensity dependence and the sharply concentrated emission profile in time are caused by the characteristic structure of the macropulse, which is densely packed with a large number of micropulses. Because the period of micropulse repetition (350 ps) is much shorter than the intrinsic carrier decay time (3 ns), the ionization and relaxation event is not terminated within a single micropulse but is repeated to be amplified pulse by pulse. It was proved that when a single electron is magnified to $1 + Q \simeq 1.1$ electrons by irradiation of a single micropulse, the sharply concentrated emission profile and nearly the 100th power of excitation-intensity dependence take place.

References

1) R. E. Russo: Appl. Spectrosc. **49** (1995) 14A.
2) N. Mori, T. Takahashi, T. Kambayashi, H. Kubo, C. Hamaguchi, L. Eaves, C. T. Foxon, A. Patane, and M. Henini: Physica B **314** (2002) 431.
3) T. Mitsuyu, T. Suzuki, and T. Tomimasu: Nucl. Instrum. Methods Phys. Res., Sect. B **144** (1998) 172.
4) M. Yasumoto, N. Umesaki, T. Tomimasu, T. Takii, Y. Kanazawa, and A. Zako: Nucl. Instrum. Methods Phys. Res., Sect. B **144** (1998) 176.
5) H. Kuroda: *Proc. Int. Symp. Infrared Free Electron Laser and Its Application, Kyoto, 1987*, Jpn. J. Appl. Phys., **41** (2002) Suppl. 41-1, p. 1.
6) T. Tomimasu, K. Saeki, Y. Miyauchi, E. Oshita, S. Okuma, K. Wakita, A. Kobayashi, T. Suzuki, A. Zako, S. Nishihara, A. Koga, K. Wakisaka, H. Tongu, A. Nagai, and M. Yasumoto: Nucl. Instrum. Methods Phys. Res., Sect. A **375** (1996) 626.
7) Y. Ogi, T. Endo, K. Tsukiyama, H. Kondoh, K. Tono, Y. Ogawa, Y. Hamada, T. Ohta, and H. Kuroda: *Proc. Int. Symp. Infrared Free Electron Laser and Its Application, Kyoto, 1987*, Jpn. J. Appl. Phys. **41** (2002) Suppl. 41-1, p. 108.
8) K. Tono, K. Bito, H. Kondoh, T. Ohta, and K. Tsukiyama: J. Chem. Phys. **125** (2006) 224305.
9) G. E. Hite, D. T. F. Marple, M. Aven, and B. Segall: Phys. Rev. **156** (1967) 850.
10) A. G. Markelz, N. G. Asmar, B. Brar, and E. G. Gwinn: Appl. Phys. Lett. **69** (1996) 3975.
11) H. K. Jung, K. Taniguchi, and C. Hamaguchi: J. Appl. Phys. **79** (1996) 2473.
12) P. H. Bucksbaum, R. R. Freeman, M. Bashkansky, and T. J. McIlrath: J. Opt. Soc. Am. B **4** (1987) 760.
13) J. Z. Zheng and J. W. Allen: J. Appl. Phys. **67** (1990) 2060.
14) J. Z. Zheng, J. W. Allen, D. E. Spence, W. E. Sleat, and W. Sibbett: Appl. Phys. Lett. **62** (1993) 64.
15) E. Yablonovitch and N. Bloembergen: Phys. Rev. Lett. **29** (1972) 907.
16) B. Kochman, K. Yoem, and J. Singh: Appl. Phys. Lett. **68** (1996) 1936.